Solution Viscosity of a Moderately Stiff Polymer: Cellulose Tris(phenyl carbamate)

Takahiro Sato* and Mitsuharu Hamada†

Department of Macromolecular Science, Osaka University, 1-1 Machikaneyama-cho, Toyonaka, Osaka 560-0043, Japan

Akio Teramoto

Research Organization of Science and Engineering and Faculty of Science and Engineering, Ritsumeikan University, Nojihigashi 1-1-1, Kusatsu, Siga 525-8577, Japan

Received April 7, 2003; Revised Manuscript Received June 23, 2003

ABSTRACT: Zero-shear viscosities η_0 of tetrahydrofuran solutions of cellulose tris(phenyl carbamate) (CTC), a moderately stiff polymer of persistence length $q = 10.5$ nm, were measured as a function of the polymer concentration c and molecular weight M. The molecular weight dependence of η_0 at high concentration is definitely stronger than that of flexible polymers, reflecting the chain stiffness of CTC. The η_0 data for higher molecular weight samples are favorably compared with the fuzzy-cylinder model theory, but it is necessary to consider up to the terms in c^2 in the intermolecular hydrodynamic interaction (HI) when the M of CTC is low. When compared among polymers of the same contour length but different stiffness, the intermolecular HI becomes more important with decreasing q.

Introduction

Solution viscosity is very high for stiff polymers even at low concentrations. For example, xanthan gum,[1,2] scureloglucan,[3,4] and succinoglycan,[5,6] which are known to be very effective viscosity-enhancing agents added into foods or industrial materials, are all rigid helical polysaccharides with the persistence length q of 50−200 nm, and their rigidity is the origin of the viscosity enhancement. The high viscosities of polymer solutions are induced by intermolecular interactions among polymer chains, which are usually divided into two parts: the short-range entanglement interaction and long-range hydrodynamic interaction (HI). With increasing the polymer chain stiffness, the entanglement effect on the solution viscosity strongly increases,[7] while the effect of the latter interaction becomes minor.[8] We have demonstrated that the entanglement effect is accurately described by the fuzzy-cylinder theory for such solutions of stiff polymers of medium molecular weights.[7]

On the other hand, with decreasing the polymer chain stiffness, we may expect a different situation on the polymer solution viscosity. Previous studies[9−11] on zero-shear viscosities η_0 of poly(n-hexyl isocyanate) (PHIC) solutions with q of ca. 20−40 nm showed that the fuzzy-cylinder theory becomes less accurate in very low and high molecular weight regions. The disagreements may be ascribed to effects of the intermolecular HI and of the reptation-like motion in the low and high molecular weight regions, respectively. Including the intermolecular HI effect in the fuzzy-cylinder theory,[10] a good agreement was recovered for low molecular weight PHIC samples.

In the present study, we have investigated solution viscosities of a cellulose derivative, cellulose tris(phenyl carbamate) (CTC), with a moderate stiffness ($q = 10.5$ nm) between typical stiff and flexible polymers. Since its molecular characteristics have been already studied previously,[12] CTC is suitable for quantitative arguments on the solution viscosity. Comparing η_0 for polymers of largely different stiffness, we have examined the chain flexibility effect on η_0 in detail, especially on roles of entanglement and hydrodynamic interactions in η_0.

† Present address: Procter & Gamble Far East, Inc., 17, Koyo-cho, Naka 1-chome, Higashinada-ku, Kobe 658-0032, Japan.

* Corresponding author: Tel +81-6-6850-5461; Fax +81-6-6850-5461; e-mail tsato@chem.sci.osaka-u.ac.jp.

Experimental Section

Seven fractionated CTC samples were used for viscosity measurements. Among the samples, five samples (F12, F14, F17, F19, and F23) were the same as those used in a previous study,[12] and two samples (Q1-2 and K3-3) were newly prepared in the same method as previously. Molecular characteristics of all the samples are listed in Table 1. For the newly prepared samples, the viscosity-average molecular weight M_v was estimated from the intrinsic viscosity [η] in tetrahydrofuran (THF) at 25 °C by using the [η]−molecular weight relation reported previously.[12] In the following, both M_v and the weight-average molecular weight M_w are denoted simply as M.

For all the samples (except for sample F23), their ratios of the weight- to number-average molecular weight (M_w/M_n) estimated by GPC are less than 1.1 (cf. the seventh column of Table 1), guaranteeing narrow molecular weight distributions of the samples used. Degrees of substitution of the CTC samples estimated by elemental analysis are listed in the eighth column of Table 1. The results indicate the full substitution on hydroxyl groups in the cellulose chain.

The contour length L and the number of Kuhn's statistical segments N for each sample in THF were calculated from M by using the molecular weight per unit contour length $M_L = 1040\ \mathrm{nm}^{-1}$ and the persistence length $q = 10.5$ nm determined previously.[12] Those results are also listed in Table 1. As shown previously, the intramolecular excluded-volume effect is negligible for CTC in THF at $M < \sim 3 \times 10^5$.[12] Thus, we do not consider this effect in what follows.

Shear viscosities η of THF solutions of CTC samples at 25 °C were measured at different shear rates and polymer concentrations by a magnetically controlled ball viscometer (Iwamoto Co. Ltd., Kyoto, Japan) or by a four-bulb low-shear-capillary viscometer, both of which were used in previous studies; see ref 9 for the detailed procedure. Zero-shear viscosities η_0 were obtained by extrapolating η obtained to the zero-shear rate. The intrinsic viscosity [η] and the Huggins coefficient k' of each CTC sample were determined by viscometry for dilute solutions of the CTC sample using a conventional capillary viscometer (cf. the fifth and sixth columns of Table 1).

10.1021/ma030204a CCC: $25.00
Published on Web 08/15/2003

Table 1. Molecular Characteristics of CTC Samples Used (in THF at 25 °C)

sample	$M_w/10^4$	L/nm[b]	N[c]	$[\eta]$/cm^3 g^{-1}	k'	M_w/M_n[d]	DS[e]
Q1-2	35[a]	340	16	254	0.38	1.09	3.1
F12	23.2	223	10.6	177	0.37	1.07	3.1
F14	15.0	144	6.87	119	0.35	1.05	3.0
K3-3	8.2[a]	79	3.7_5	69.9	0.36	1.07	3.0
F17	6.42	61.7	2.94	48.3	0.39	1.07	3.2
F19	4.06	39.0	1.86	31.8	0.42	1.08	2.8
F23	1.91	18.4	0.875	0.145	0.46		3.0

[a] Viscosity-average molecular weight estimated from $[\eta]$ in THF (25 °C) with the established $[\eta]-M_w$ relations.[12] [b] Calculated from M_w with the molecular weight per unit contour length $M_L = 1040$ nm^{-1}. [c] Calculated from L with the persistence length $q = 10._5$ nm. [d] Estimated by GPC with the calibration curve constructed by narrow-distribution CTC samples of which molecular weights were determined by light scattering. [e] Degree of substitution estimated by elemental analysis.

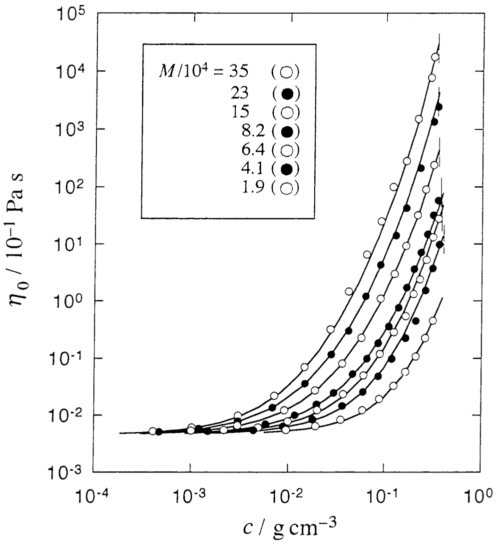

Figure 1. Double-logarithmic plots of the zero-shear viscosity η_0 vs the polymer mass concentration c for THF solutions of CTC at 25 °C.

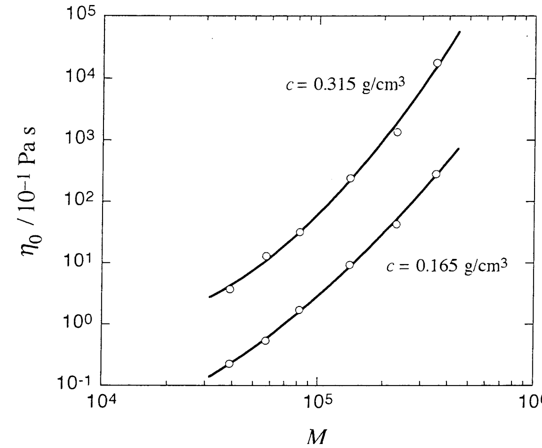

Figure 2. Double-logarithmic plots of the zero-shear viscosity η_0 vs the polymer molecular weight M for THF solutions of CTC with two different polymer concentrations.

Results

Figure 1 shows double-logarithmic plots of the zero-shear viscosity η_0 vs the polymer mass concentration c for THF solutions of seven CTC samples at 25 °C. In the figure, vertical segments attached to experimental curves indicate phase boundary concentrations c_I where the cholesteric phase starts to appear, which were estimated from c_I data obtained previously.[13] The data points of η_0 follow curves concave upward up to c near c_I. This non-power-law behavior is characteristic of stiff-chain polymer solutions.[2,7,14,15]

Figure 2 shows double-logarithmic plots of η_0 vs the molecular weight M for CTC solutions at two fixed c. The data points follow curves concave upward with the slopes of 4.7 (for $c = 0.315$ g/cm^3) and 3.7 (for $c = 0.165$ g/cm^3) at high M regions. Those slopes for CTC solutions are larger than the well-known exponent 3.4 for solution viscosities of entangled flexible polymers,[16,17] and the large exponent is characteristic of stiff polymer solutions.[2,7,14,15]

In Figure 3, relative viscosities η_r (i.e., η_0 divided by the solvent viscosity $\eta^{(S)}$) for five polymer solution systems with different chain stiffness but almost the same contour length L ($\approx$200 nm)[18] are plotted against the molar concentration c/M. The chain stiffness can be expressed in terms of q; q values of schizophyllan (a triple-helical polysaccharide), xanthan (a double-helical polysaccharide), poly(n-hexyl isocyanate) (PHIC), CTC, and polystyrene are 200, 100, 37 (in toluene), 10.5, and 1 nm,[19] respectively.[7,20] It can be seen that η_r steeply

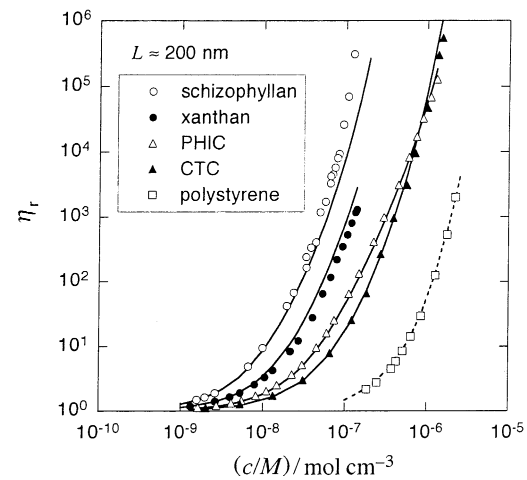

Figure 3. Relative viscosities η_r of five polymer solution systems with different chain stiffness, plotted against the molar concentration c/M: (△) schizophyllan (a triple-helical polysaccharide) in water at 25 °C ($q = 200$ nm; $L = 210$ nm),[14] (▲) xanthan (double-helical ionic polysaccharide) in 0.1 M aqueous NaCl at 25 °C ($q = 100$ nm; $L = 190$ nm),[2] (○) poly(n-hexyl isocyanate) (PHIC) in toluene at 25 °C ($q = 37$ nm; $L = 210$ nm),[11] (●) CTC in THF at 25 °C ($q = 10.5$ nm; $L = 220$ nm), (□) polystyrene in cyclohexane at 34.5 °C ($q = 1$ nm; $L = 340$ nm).[27] Solid curves: the fuzzy-cylinder theory; dotted curve for polystyrene solutions: eye guide.

increases at lower molar concentrations for stiffer polymers. This is a clear demonstration that the polymer chain stiffness is an essential factor in the polymer solution viscosity. However, we can see that η_r of CTC solutions becomes higher than that of PHIC solutions at high concentrations. This viscosity inversion will be discussed in the next section.

Discussion

Previous studies[7,10,11,21] showed that solution viscosities of stiff polymers were favorably compared with the dynamical theory based on the fuzzy-cylinder model unless the molecular weight of the polymer is too large. Here we compare the Huggins coefficient k' and also η_0 data for CTC solutions with the fuzzy-cylinder theory. In the theory, polymer chains in solution are represented by the fuzzy cylinder model. The effective length L_e of the fuzzy cylinder is identified with the root-mean-square end-to-end distance of the polymer chain ($= L[N^{-1} - (1 - e^{-2N})/2N^2]^{1/2}$, where N is the number of Kuhn's statistical segments), and the effective diameter d_e of the fuzzy cylinder is also calculated from L, N, and the diameter d of the polymer chain.[7] As shown previously,[10] k' can be written in the form

$$k' = k'_{HI} + k'_{EI} \tag{1}$$

where k'_{HI} and k'_{EI} are the contributions of the intermolecular hydrodynamic interaction (HI) and of the entanglement interaction to k', respectively. The latter can be calculated theoretically by[10]

$$k'_{EI} \equiv \frac{3}{2\sqrt{1350}} \frac{L_e^{\,4} N_A}{[\eta]ML} f_r(d_e/L_e)\gamma\chi^2 (F_{||0}/F_{r0})^{1/2} \tag{2}$$

Here $f_r(d_e/L_e)$ is a known function of d_e/L_e, γ and χ are hydrodynamic parameters calculated from the axial ratio p of the polymer chain, and $F_{||0}$ and F_{r0} are another hydrodynamic parameters related to the longitudinal and rotational diffusion coefficients at infinite dilution calculated from p and N (N_A: the Avogadro constant).[7,21]

Using the wormlike-cylinder parameters determined previously (q = 10.5 nm and d = 2.2 nm),[12] we can calculate theoretical values of k'_{EI} for CTC in 25 °C THF as a function of L, which is indicated by the solid curve in Figure 4.[22] Furthermore, from the experimental k' and the theoretical k'_{EI}, we can estimate k'_{HI} using eq 1, which are shown by circles in Figure 4; the filled circles are k'_{HI} for the CTC samples used in this study, and unfilled circles indicate k'_{HI} obtained from k' data for other samples presented previously.[12] The contribution of the intermolecular HI to k' takes a minimum at $L \approx 100$ nm (or $M \approx 2 \times 10^5$). A similar L dependence of k'_{HI} has been already reported for toluene solutions of PHIC[11] (cf. triangles in Figure 4), but values of k'_{HI} for PHIC are smaller than those of CTC at the same L except at very short L; k'_{HI} for PHIC at $L \approx 100$ nm take slightly negative values maybe due to inaccuracy in k'_{EI}. Since k'_{HI} for stiffer polymers like schizophyllan and xanthan are negligibly small except for very short chains,[10] we may conclude that the intermolecular HI is more important in the solution viscosity for less stiff polymers if p is not small.

According to the previous formulation,[10] the zero-shear viscosity η_0 is written as

$$\eta_0 = \eta^{(S)} + \eta^{(S)}[\eta]c\left[1 + \frac{3}{4}\gamma\chi^2\left(\frac{\hat{D}_{r0}}{D_r} - 1\right)\right]h_\eta(c) \tag{3}$$

where $\eta^{(S)}$ is the solvent viscosity, D_r and $\hat{D}_{r0}$ are the rotational diffusion coefficient with and without perturbed by the entanglement effect, respectively, and $h_\eta(c)$ is the viscosity enhancement factor by the intermolecular HI given below. The entanglement effect on $\hat{D}_{r0}/D_r$ was formulated by the mean-field Green function method (cf. eq 2 in ref 10) as a function of c and M. Since entanglements among stiff-polymer chains are mainly released by the longitudinal diffusion of the chains, the equation of $\hat{D}_{r0}/D_r$ includes the longitudinal diffusion coefficient $D_{||}$, which is perturbed by the head-on collision with the surrounding molecules (the jamming effect) and was previously formulated on the basis of the hole theory.[7,21] In this theory, the probability of the collision is expressed by the similarity ratio λ^* between the fuzzy cylinder and the critical hole for the longitudinal diffusion, and thus the equation of $\hat{D}_{r0}/D_r$ contains λ^* as an adjustable parameter. On the other hand, we[10,11] have previously demonstrated that viscosities of PHIC solutions can be favorably compared with eq 3, by taking into account the effect of the intermolecular HI up to the first order of c or by expressing $h_\eta(c)$ by

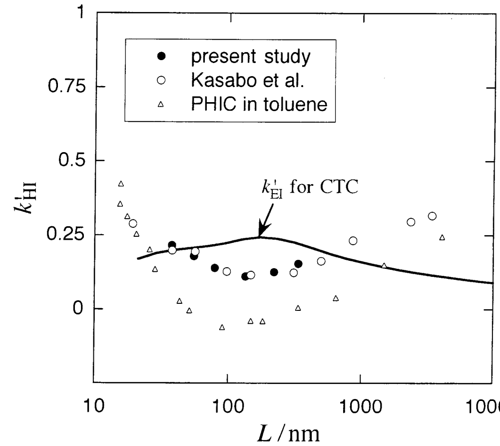

Figure 4. Contributions of the entanglement interaction k'_{EI} and the intermolecular hydrodynamic interaction k'_{HI} to the Huggins coefficient for THF solutions of CTC: the solid curve, k'_{EI} calculated for CTC in THF by the fuzzy-cylinder theory (eq 2); filled and unfilled circles, k'_{HI} for samples used in the present and previous studies,[12] respectively; triangles, k'_{HI} for poly(n-hexyl isocyanate) in toluene at 25 °C.[11]

$$h_\eta(c) = 1 + k'_{HI}[\eta]c \tag{4}$$

By using eq 4 along with k'_{HI} given in Figure 4 and choosing changing λ^* to be 0.04, we obtain solid curves in Figure 5 from eq 3, which nicely fit η_0 data for CTC solutions except for the two lowest molecular weight samples. The value of λ^* chosen is close to that chosen for PHIC solutions ($\lambda^* = 0.03$)[11] but smaller than those for stiffer polymer solutions of schizophyllan and xanthan ($\lambda^* \approx 0.1$).[7,21] Solid curves in Figure 3 for four stiff or semiflexible polymer solution systems are also drawn by the same theory.[23] The stiffer the polymer chain is, the larger the value of L_e is at equal L.[7] Because $\hat{D}_{r0}/D_r$ in eq 3 contains a term proportional to L_e,[4] the increase in L_e strongly enhances the viscosity. On the other hand, the viscosity inversion observed for CTC and PHIC solutions at a high polymer concentration is owing to stronger intermolecular HI for the former solution, as shown in Figure 4.

In Figure 5, the disagreement between the theory (solid curves) and experiment for the two lowest molecular weight CTC samples at higher concentration regions may arise from higher order terms of c in $h_\eta(c)$, being neglected in eq 4. Considering up to the second-order term, we write

$$h_\eta(c) = 1 + k'_{HI}[\eta]c + k''_{HI}([\eta]c)^2 \tag{5}$$

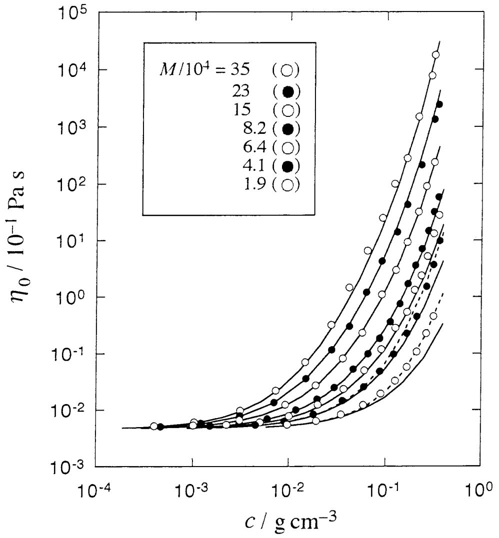

Figure 5. Comparison between the fuzzy-cylinder theory and experiment for zero-shear viscosities of THF solutions of CTC: solid curves, calculated by eqs 3 and 4; dashed curves, calculated by eqs 3 and 5.

For suspensions of rigid spheres where the entanglement effect vanishes (or $\hat{D}_{r0}/D_r = 1$ in eq 3), theories predict that $k''_{HI}/k'^{2}_{HI} \approx 1$,[24,25] but experimental results indicate a larger contribution of the second-order term ($k''_{HI}/k'^{2}_{HI} \approx 6.5$).[26] For CTC solutions, if k''_{HI}/k'^{2}_{HI} are chosen to be 2.4 and 1.1 respectively for samples F23 ($p = 8.7$) and F19 ($p = 17$), eq 3 along with eq 5 gives us dashed curves in Figure 5, which fit to experimental data for the two samples. The parameter k''_{HI} seems to be a decreasing function not only of p but also of q because the second-order term was not detectable in solution viscosity of PHIC even at p as small as 10.[11]

As shown in previous papers,[11] the fuzzy-cylinder theory failed to describe solution viscosity data for PHIC with $N \gtrsim 20$, and this failure was ascribed to the reptation-like motion of polymer chains taking coiled conformations in concentrated solutions which is not incorporated in the fuzzy-cylinder theory. Since N of all CTC samples examined in this study are smaller than 20, the effect of the reptation motion may be unimportant. Good agreements between theory and experiment for higher molecular weight CTC samples shown in Figure 5 demonstrate that the fuzzy-cylinder theory is applicable even for semiflexible polymer solutions with q as small as 10 nm when $N \lesssim 20$.

Conclusions

The viscosity enhancement in polymer solutions can be argued in terms of the two effects of the entanglement and of the intermolecular hydrodynamic interaction (HI). The former effect becomes stronger with increasing the polymer-chain stiffness but weaker with decreasing the axial ratio p of the polymer chain; it vanishes for spheres ($p = 1$). As demonstrated above and also in previous papers,[7,10,11,21] the entanglement effect in semiflexible or stiff polymer solutions can be successfully described by the fuzzy-cylinder theory if N is not so large.

The effect of the intermolecular HI plays an important role in the solution viscosity when the stiffness or the axial ratio of the polymer chain decreases. In the present study, the contribution of this effect to η_0 is expressed by the phenomenological eq 5 which includes up to the second-order term of the polymer concentration with two hydrodynamic parameters k'_{HI} and k''_{HI}. We have determined k''_{HI} by fitting the theory to experimental data of η_0. Theoretical calculations of k''_{HI} have not been performed for polymer solutions yet.

Acknowledgment. This work was supported by a Grant-in-Aid for Scientific Research from the Ministry of Education, Science, Sports, and Culture of Japan and CREST of Japan Science and Technology Corp. A. T. thanks Yamashita Construction Design Inc. for the Chair-Professorship at Ritsumeikan University.

References and Notes

(1) Sato, T.; Norisuye, T.; Fujita, H. *Macromolecules* **1984**, *17*, 2696.
(2) Takada, Y.; Sato, T.; Teramoto, A. *Macromolecules* **1991**, *24*, 6215.
(3) Yanaki, T.; Norisuye, T. *Polym. J.* **1981**, *13*, 1135.
(4) Yanaki, T.; Norisuye, T. *Polym. J.* **1983**, *15*, 389.
(5) Harada, T.; Harada, A. In *Polysaccharides in Medical Application*; Dumitriu, S., Ed.; Marcel Dekker: New York, 1996.
(6) Kido, S.; Nakanishi, T.; Norisuye, T.; Kaneda, I.; Yanaki, T. *Biomacromolecules* **2001**, *2*, 952.
(7) Sato, T.; Teramoto, A. *Adv. Polym. Sci.* **1996**, *126*, 85.
(8) Muthukumar, M.; Edwards, S. F. *Macromolecules* **1983**, *16*, 1475.
(9) Ohshima, A.; Kudo, H.; Sato, T.; Teramoto, A. *Macromolecules* **1995**, *28*, 6095.
(10) Sato, T.; Ohshima, A.; Teramoto, A. *Macromolecules* **1998**, *31*, 3094.
(11) Ohshima, A.; Yamagata, A.; Sato, T.; Teramoto, A. *Macromolecules* **1999**, *32*, 8645.
(12) Kasabo, F.; Kanematsu, T.; Nakagawa, T.; Sato, T.; Teramoto, A. *Macromolecules* **2000**, *33*, 2748.
(13) Sato, T.; Shimizu, T.; Kasabo, F.; Teramoto, A. *Macromolecules* **2003**, *36*, 2939.
(14) Enomoto, H.; Einaga, Y.; Teramoto, A. *Macromolecules* **1984**, *17*, 1573.
(15) Enomoto, H.; Einaga, Y.; Teramoto, A. *Macromolecules* **1985**, *18*, 2695.
(16) Ferry, J. D. *Viscoelastic Properties of Polymers*, 3rd ed.; John Wiley & Sons: New York, 1980.
(17) Doi, M.; Edwards, S. F. *The Theory of Polymer Dynamics*; Clarendon Press: Oxford, 1986.
(18) For lack of reference data, we plot η_0 for polystyrene of L = 340 nm in Figure 3; the η_0 curve for polystyrene with L = 200 nm would be shifted to the higher concentration side.
(19) To be consistent with other stiff polymers, the chain stiffness of polystyrene is expressed in terms of the persistence length of the wormlike chain model[28] instead of the stiffness parameter of the helical wormlike chain model.[29]
(20) Fujita, H. *Polymer Solutions*; Elsevier: Amsterdam, 1990.
(21) Sato, T.; Takada, Y.; Teramoto, A. *Macromolecules* **1991**, *24*, 6220.
(22) Equation 10 in ref 10 contains two additional parameters N^* and Δ in the f_r function. We have assumed that N^* and Δ for CTC are identical with those for poly(*n*-hexyl isocyanate) (PHIC) previously determined to be $N^* = \Delta = 4$. Since k' and η_0 are insensitive to values of N^* and Δ, variances in N^* and Δ do not so much affect final results.
(23) Agreement between the theory and experiment for schizophyllan and xanthan solutions seems to be less satisfactory. We determined the λ^* parameter for the two systems so as to fit η_0 data for different molecular weight samples equally well by the fuzzy-cylinder theory.[21]
(24) Frisch, H. L.; Simha, R. In *Rheology*; Eirich, F. R., Ed.; Academic Press: New York, 1956.
(25) Beenakker, C. W. J. *Physica* **1984**, *128A*, 48.
(26) de Kruif, C. G.; van Iersel, E. M. F.; Vrij, A.; Russel, W. B. *J. Chem. Phys.* **1985**, *83*, 4717.
(27) Hamada, K. BS Thesis, Osaka University, 1985.
(28) Norisuye, T.; Fujita, H. *Polym. J.* **1982**, *14*, 143.
(29) Yamakawa, H. *Helical Wormlike Chains in Polymer Solutions*; Springer-Verlag: Berlin, 1997.

MA030204A